

Single electron capture in fast ion-atom collisions

Nenad Milojević

Department of Physics, Faculty of Sciences and Mathematics, University of Niš, P.O.Box 224,
18000 Niš, Serbia

E-mail: nenad81@pmf.ni.ac.rs

Abstract. Single-electron capture cross sections in collisions between fast bare projectiles and heliumlike atomic systems are investigated by means of the four-body boundary-corrected first Born (CB1-4B) approximation. The prior and post transition amplitudes for single charge exchange encompassing symmetric and asymmetric collisions are derived in terms of two-dimensional real integrals in the case of the prior form and five-dimensional quadratures for the post form. The dielectronic interaction $V_{12} = 1/r_{12} \equiv 1/|\mathbf{r}_1 - \mathbf{r}_2|$ explicitly appears in the complete perturbation potential V_f of the post transition probability amplitude T_{if}^+ . An illustrative computation is performed involving state-selective and total single capture cross sections for the p – He (prior and post form) and He²⁺, Li³⁺, Be⁴⁺, B⁵⁺, C⁶⁺ – He (prior form) collisions at intermediate and high impact energies. We have also studied differential cross sections in prior and post form for single electron transfer from helium by protons. The role of dynamic correlations is examined as a function of increased projectile energy. Detailed comparisons with the measurements are carried out and the obtained theoretical cross sections are in reasonable agreement with the available experimental data.

1. Introduction

The investigation and differentiation electron capture from atomic and molecular targets by the impact of fast ions has been a topic of considerable interest in atomic collision physics for many years. This occurs because of the critical importance of charge transfer cross sections in a number of applications in astrophysics, plasma physics, thermonuclear fusion research and medical accelerators for hadron radiotherapy. In the present work we report on our theoretical investigation of single electron capture from heliumlike atomic systems interacting with bare projectiles (p, He²⁺, Li³⁺, Be⁴⁺, B⁵⁺, and C⁶⁺), with all four particles actively participating in these processes. Hence, this is a pure four-body problem that involves laborious analytical and numerical theoretical computations within any type of first order approximations. Total and differential cross sections in prior and post form are calculated by using four-body boundary-corrected first Born (CB1-4B) approximation. The first Born approximation with the correct boundary conditions has been introduced within the three-body formalism [1]. On the other hand, the CB1-4B method was adapted and applied to single-electron capture [2]-[4].

The CB1-4B method is a fully quantum mechanical four-body formalism, and it explicitly considers each individual particle and all the interactions among them in the collision under investigation. It strictly preserves the correct boundary conditions in both collisional channels, and it is well known that the boundary conditions (the asymptotic convergence problem [5]-[9]) are of essential importance for atomic collisions whenever the aggregates are charged in the asymptotic channels.



Atomic units will be used throughout unless otherwise stated.

2. Theory

We consider single electron capture in collisions of a completely stripped projectile with a helium-like target:

$$X^{Z_{P^+}} + (Z_T; e_1, e_2)_{1s^2} \longrightarrow (X^{Z_{P^+}}, e_1)_{nlm} + (Z_T, e_2)_{1s}, \quad (1)$$

where Z_K is the charge of the K th nucleus ($K = P, T$) and nlm is the usual set of three quantum numbers of hydrogenlike atomic systems. Here, the parentheses symbolize the bound states. Let \vec{s}_1 and \vec{s}_2 (\vec{x}_1 and \vec{x}_2) be the position vectors of the first and second electron (e_1 and e_2) relative to the nuclear charge of the projectile Z_P (target Z_T), respectively. Further, let \vec{R} be the position vector of Z_T with respect to Z_P .

The prior and post form of the transition amplitude for process (1) in the CB1-4B approximation without the term $(\rho v)^{2iZ_P(Z_T-2)/v}$ read as [2]:

$$T_{if}^{\pm}(\vec{\eta}) = \int \int \int d\vec{x}_1 d\vec{x}_2 d\vec{R} \varphi_{nlm}^*(\vec{s}_1) \varphi_{100}^*(\vec{x}_2) V^{\pm} \varphi_i(\vec{x}_1, \vec{x}_2) e^{-i\vec{\alpha} \cdot \vec{R} - i\vec{v} \cdot \vec{x}_1} (vR + \vec{v} \cdot \vec{R})^{i\xi}, \quad (2)$$

$$V^+ \equiv V_f = \Delta V_{P2} + \Delta V_{T1} + \Delta V_{12}, \quad \Delta V_{12} = V_{12} - V_{12}^{\infty}, \quad V_{12} = \frac{1}{r_{12}}, \quad V_{12}^{\infty} = \frac{1}{x_1}, \quad (3)$$

$$V^- \equiv V_i = \Delta V_{P1} + \Delta V_{P2}, \quad (4)$$

where

$$\Delta V_{Pi} = Z_P \left(\frac{1}{R} - \frac{1}{s_i} \right), \quad (i = 1, 2), \quad \Delta V_{T1} = (Z_T - 1) \left(\frac{1}{R} - \frac{1}{x_1} \right). \quad (5)$$

Here, $\xi = (Z_P - Z_T + 1)/v$ where v is the velocity of the projectile and $\vec{\rho} = \vec{R} - \vec{Z}$, $\vec{\rho} \cdot \vec{Z} = 0$. The vector of the distance between the two electrons e_1 and e_2 is denoted by $\vec{r}_{12} = \vec{x}_1 - \vec{x}_2 = \vec{s}_1 - \vec{s}_2$, and we have $r_{12} = |\vec{r}_{12}|$. The momentum transfer $\vec{\alpha}$ and transverse momentum transfer $\vec{\eta}$ are defined by:

$$\vec{\alpha} = \vec{\eta} - (v/2 - \Delta E/v)\hat{v}, \quad \vec{\eta} = (\eta \cos \phi_{\eta}, \eta \sin \phi_{\eta}, 0), \quad \vec{\eta} \cdot \vec{v} = 0, \quad (6)$$

where $\Delta E = E_i - E_f$ with E_i being the binding energy of the two-electron target and $E_f = -Z_P^2/[2n^2] - Z_T^2/2$. The function $\varphi_i(\vec{x}_1, \vec{x}_2)$ denotes the two-electron ground state wave function of the atomic system $(Z_T; e_1, e_2)_{1s^2}$. The functions $\varphi_{nlm}(\vec{s}_1)$ and $\varphi_{100}(\vec{x}_2)$ in Eq. (2) represent the bound state wave functions of the hydrogen-like atomic systems $(X^{Z_{P^+}}, e_1)_{nlm}$ and $(Z_T, e_2)_{1s}$, respectively.

The original nine-dimensional integral for transition amplitude can be reduced to a two-dimensional integral and five-dimensional integral over real variables in prior [3] and post [4] form, respectively.

The differential (DCS) and total (TCS) cross sections (prior and post form) in the CB1-4B method are given by:

$$\frac{dQ_{if}^{\pm}}{d\Omega} \left(\frac{a_0^2}{sr} \right) = \frac{\mu^2}{4\pi^2} |T_{if}^{\pm}(\vec{\eta})|^2, \quad Q_{if}^{\pm}(a_0^2) = \int \frac{dQ_{if}^{\pm}}{d\Omega} d\Omega = \frac{1}{2\pi v^2} \int_0^{\infty} d\eta \eta |T_{if}^{\pm}(\vec{\eta})|^2, \quad (7)$$

where $\mu_i \simeq \mu_f \simeq \mu = M_P M_T / (M_P + M_T)$ is the reduced mass of the incident and target nuclei with the mass M_P and M_T respectively. All numerical integrations are performed by means of the Gauss-Legendre and Gauss-Mehler quadrature. The numbers of integration points are varied until convergence to two decimal places has been attained for state-selective and total cross sections.

Total cross sections $Q^\pm(\Sigma)$ for electron capture into all the final states for reaction (1) are obtained by applying the Oppenheimer (n^{-3}) scaling law [10, 11] via:

$$Q_{\text{tot}}^\pm \equiv \sum_{n=1}^{\infty} Q_n^\pm \simeq Q^\pm(\Sigma_N) = \sum_{n=1}^{N-1} Q_n^\pm + \gamma(3, N-1)Q_N^\pm, \quad (8)$$

where

$$\gamma(3, N) = 1 + (N+1)^3 \zeta(3) - \sum_{n=1}^{N+1} \left(\frac{N+1}{n} \right)^3, \quad (9)$$

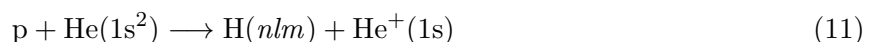
with $\zeta(3)$ being the Riemann zeta function $\zeta(3) = \sum_{n=1}^{\infty} n^{-3} \approx 1.202$, and partial cross sections

$$Q_n^\pm = \sum_{l=0}^{n-1} Q_{nl}^\pm, \quad Q_{nl}^\pm = \sum_{m=-l}^{+l} Q_{nlm}^\pm. \quad (10)$$

The computations are stopped when the total cross sections Q_{tot}^\pm become insensitive to inclusion of more partial (state-selective) cross sections Q_n^\pm .

3. Results and discussions

First we shall examine electron capture from He($1s^2$) by proton (asymmetric reaction):



in the energy range from 20 to 10000 keV. The total CB1-4B cross sections in the prior form obtained with the complete perturbation V_i by using Eq. (8) (where is $N = 4$):

$$Q_{\text{tot}}^- \simeq Q^-(\Sigma_4) = Q_1^- + Q_2^- + Q_3^- + 2.561Q_4^-, \quad (12)$$

are plotted in Fig.1. The full line shows the results obtained by means of the two-parameter wave function of Silverman *et al.* [12] for the ground state of the helium atom:

$$\varphi_i(\vec{x}_1, \vec{x}_2) = (N/\pi)(e^{-\alpha_1 x_1 - \alpha_2 x_2} + e^{-\alpha_2 x_1 - \alpha_1 x_2}), \quad N^{-2} = 2[(\alpha_1 \alpha_2)^{-3} + (\alpha_1/2 + \alpha_2/2)^{-6}], \quad (13)$$

whereas the dashed line represents the cross sections obtained by using uncorrelated one-parameter Hylleraas wave function [13] for the ground state of the helium atom:

$$\varphi_i(\vec{x}_1, \vec{x}_2) = (\alpha^3/\pi) e^{-\alpha(x_1+x_2)}, \quad \alpha = Z_T - 5/16. \quad (14)$$

The total cross sections obtained with these wave functions are close to each other, and the dashed curve slightly overestimates the full curve at impact energies in the range from 100 to 1000 keV, but outside this range the behaviour is the opposite. The relative difference $\chi = |Q_S^- - Q_H^-|/Q_S^-$ (where Q_S^- and Q_H^- are the present cross sections obtained by using wave

functions of Silverman *et al.* [12] and Hylleraas [13], respectively) of the prior cross sections between these wave functions does not exceed 22%. These results are seen to be in very good agreement with all the available measurements in an energy range which remarkably covers nearly three orders of magnitude.

The total cross sections for reaction (11) computed in the prior and post version of the CB1-4B method by using the four-parameter wave function of Löwdin [22] for ground state are displayed in Fig. 2. This function is given by $\varphi_i(\vec{x}_1, \vec{x}_2) = (N/\pi)(\alpha_1 e^{-\beta_1 x_1} + \alpha_2 e^{-\beta_2 x_1})(\alpha_1 e^{-\beta_1 x_2} + \alpha_2 e^{-\beta_2 x_2})$, where the normalization constants $N^{-1} = [\alpha_1^2/\beta_1^3 + \alpha_2(\alpha_2/\beta_2^3 + 16\alpha_1/(\beta_1 + \beta_2)^3)]$. The total cross sections have been obtained by summing over all contributions from the individual shells and sub-shells up to $n = 3$: $Q_{\text{tot}}^{\pm} \simeq Q^{\pm}(\Sigma_3) = Q_1^{\pm} + Q_2^{\pm} + 2.081Q_3^{\pm}$.

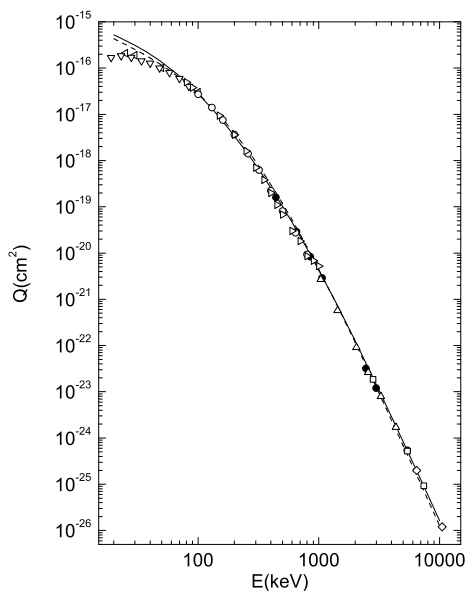


Figure 1. Total cross sections $Q^-(\Sigma_4)$ (in cm^2) as a function of the laboratory incident energy for reaction (11). The full and the dashed curves are the present cross sections obtained by using the helium ground state wave functions of Silverman *et al.* [12] and Hylleraas [13], respectively. Experimental data: ∇ Shah *et al.* [14], \triangle Schryber [15], \circ Shah and Gilbody [16], \square Horsdal-Pedersen *et al.* [17], \diamond Berkner *et al.* [18], \triangleright Williams [19], \triangleleft Martin *et al.* [20] and \bullet Welsh *et al.* [21].

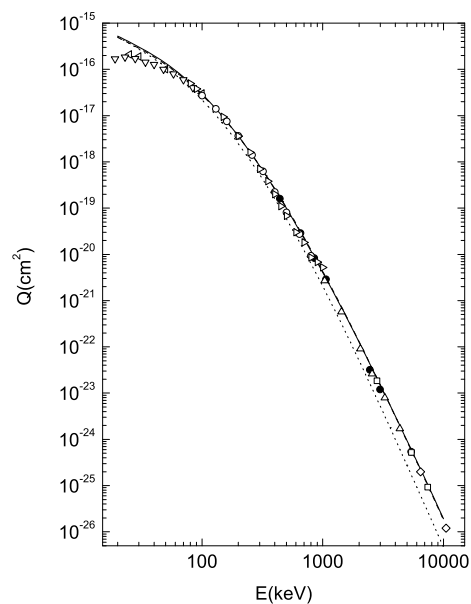


Figure 2. Total cross sections $Q^{\pm}(\Sigma_3)$ (in cm^2) as a function of the laboratory incident energy for reaction (11). The full and the dotted curves are the present cross sections $Q^+(\Sigma_3)$ in the post form with and without ΔV_{12} in V_f , respectively. The dashed curve is the present cross sections $Q^-(\Sigma_3)$ with the complete potential V_i . For all the three curves, the initial ground state of the helium atom is described by means of the Löwdin [22] orbital. Experimental data: the same as in Fig. 1.

Potential ΔV_{12} in the complete perturbation V_f from (3) represents a source of the dynamic electron correlation effect, which is included throughout $1/r_{12}$. From Fig. 2 we can see that above 100 keV, where the CB1-4B model is expected to be valid, the discrepancy between the results with the complete perturbation V_f (full line) and the corresponding cross sections without ΔV_{12} in V_f (dotted line) is increasing. These discrepancies increase even further with

augmentation of the incident energy. Such a pattern indicates that the role of the screened dynamic correlations ΔV_{12} becomes more significant at higher incident energies.

Also we examine the so-called post-prior discrepancy, which arises from the unequal perturbation potentials ($V_i \neq V_f$) in the transition amplitudes, as well as from the unavailability of the exact bound-state wave function of heliumlike atomic systems. The difference between the results for the prior and post cross sections is very small (the relative difference $\chi_p = |Q^+ - Q^{+(0)}|/Q^+$, where Q^+ and $Q^{+(0)}$ are the present cross sections for capture with and without ΔV_{12} respectively, is up to 6.6%), as can be seen in Fig. 2. This is an excellent property of the CB1-4B approximation, since the same physical assumptions are involved in the prior (dashed line) and post (full line) forms of this theory. Namely, electron-electron interaction is indirectly included through $-Z_P/s_2$ ($-Z_P/s_2 = -Z_P(1/r_{12} - \vec{r}_{12} \cdot \vec{s}_1/r_{12}^3 + \dots)$ - the Taylor series around \vec{s}_1) term in the complete potential V_i .

Differential cross sections (DCS) for single electron capture in process (11) are studied at 100 keV projectile energy.

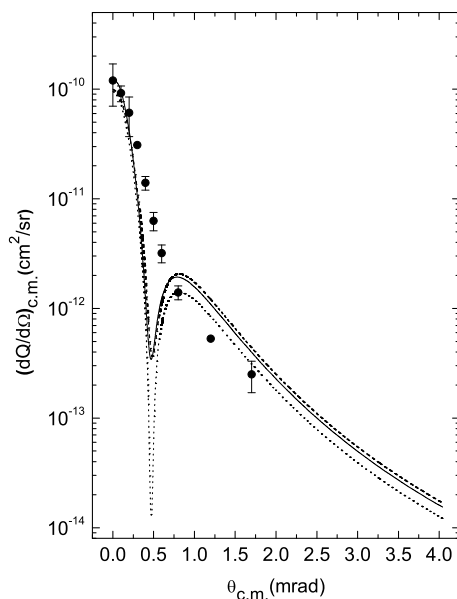


Figure 3. DCS for single electron capture for reaction (11) at 100 keV projectile energy. The full and dashed lines are the present $dQ_{tot}^-/d\Omega$ obtained by using the wave functions of Silverman *et al.* [12] and Hylleraas [13], respectively. The dotted line presents $dQ_{1s}^-/d\Omega$ with wave functions of Silverman *et al.* [12]. Exp. data: • Martin *et al.* [20].

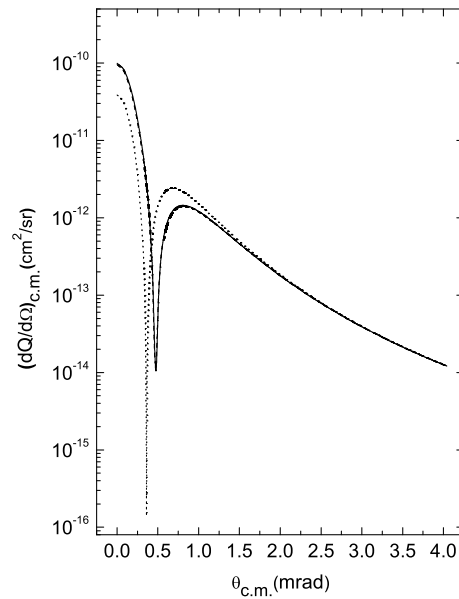


Figure 4. DCS for single electron capture for $p + \text{He}(1s^2) \rightarrow \text{H}(1s) + \text{He}^+(1s)$ collisions at 100 keV projectile impact energy. The full, dashed and dotted lines are the present $dQ_{1s}^+/d\Omega$, $dQ_{1s}^-/d\Omega$ and $dQ_{1s}^{(0)}/d\Omega$, respectively. All calculations are performed by using the helium ground-state wave functions of Silverman *et al.* [12].

Theoretical results with the available experimental data are shown in Fig. 3. Differential cross sections summed over the final states of atomic hydrogen according relation: $dQ_{tot}^-/d\Omega \simeq dQ_{1s}^-/d\Omega + dQ_{2s}^-/d\Omega + dQ_{3s}^-/d\Omega + 2.561dQ_{4s}^-/d\Omega$ are in excellent agreement with the experimental

results at scattering angles from 0 to 0.12 mrad, but at angles above 0.79 mrad theoretical cross sections overestimate the measurements. The results obtained with Hylleraas [13] wave function overestimate the results which have been calculated with Silverman *et al.* [12] function at higher scattering angles. In the same figure, the cross sections $dQ_{1s}^-/d\Omega$ for capture into the 1s state are depicted. We can see that the contribution from the excited states is more significant at higher than at lower scattering angles. Figure 4 depicts the prior and post DCS of the CB1-4B method for single-electron capture into the 1s state of atomic hydrogen using the helium wave function of Silverman *et al.* [12]. As expected, the difference between prior $dQ_{1s}^-/d\Omega$ (dashed line) and post (full line) $dQ_{1s}^+/d\Omega$ forms DCS with complete perturbation potentials V_i and V_f respectively is very small at all the considered angles. Comparing the results for the post form DCS $dQ_{1s}^{+(0)}/d\Omega$ without ΔV_{12} in V_f and results for $dQ_{1s}^-/d\Omega$ and $dQ_{1s}^+/d\Omega$, we can conclude that the screened dynamic correlations ΔV_{12} are very important at lower angles.

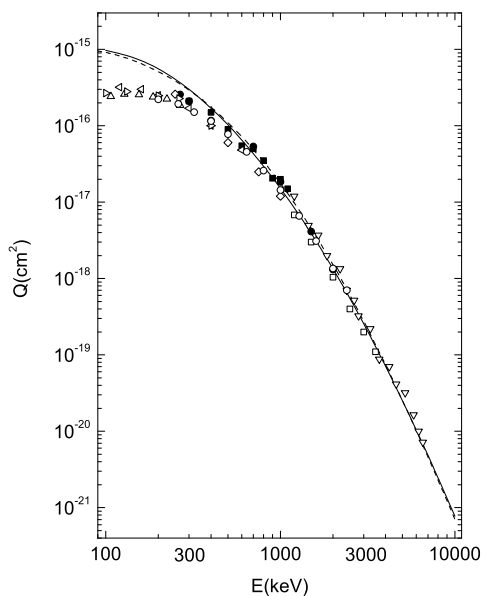


Figure 5. TCS $Q^-(\Sigma_4)$ (in cm^2) as a function of the laboratory incident energy for reaction $\text{He}^{2+} + \text{He}(1s^2) \rightarrow \text{He}^+(\Sigma) + \text{He}^+(1s)$. The full and the dashed curves are the present TCS obtained by using the wave functions of Silverman *et al.* [12] and Hylleraas [13], respectively. Exp. data: \triangle Shah *et al.* [14]; \circ Shah and Gilbody [16]; \diamond Mergel *et al.* [23]; ∇ Hvelplund *et al.* [24]; \bullet DuBois [25]; \square de Castro Faria *et al.* [26]; \blacksquare Pivovarov *et al.* [27, 28]; \triangleleft Rudd *et al.* [29]; \triangleright Alessi *et al.* [30].

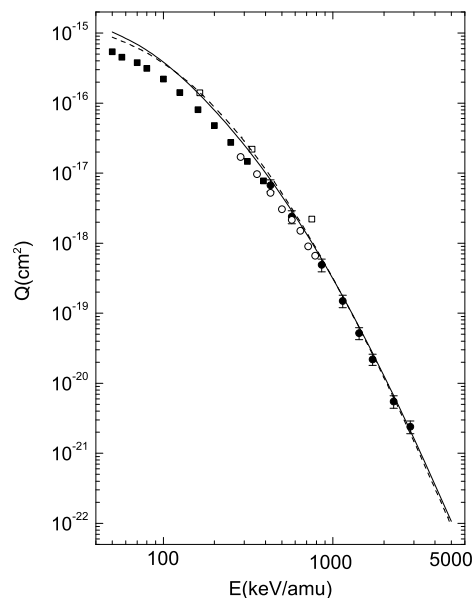


Figure 6. TCS $Q^-(\Sigma_4)$ (in cm^2) as a function of the laboratory incident energy for reaction $\text{Li}^{3+} + \text{He}(1s^2) \rightarrow \text{Li}^{2+}(\Sigma) + \text{He}^+(1s)$. The full and the dashed curves are the present TCS obtained by using the helium ground state wave functions of Silverman *et al.* [12] and Hylleraas [13], respectively. Experimental data: \blacksquare Shah and Gilbody [16]; \bullet Woitke *et al.* [31]; \circ Sant'Anna *et al.* [32]; \square Dmitriev *et al.* [33].

As seen from Figs. 3 and 4, the CB1-4B method exhibits an unphysical and experimentally unobserved dip at $\theta_{c.m.} \simeq 0.47$ mrad. This sharp dip is due to strong cancellation of the opposite contributions coming from the attractive and repulsive potentials in Eqs. (2)-(4).

Cross sections in prior form for electron capture for $\text{He}^{2+} + \text{He}(1s^2)$ collisions are calculated in the energy range from 100 to 10000 keV. These results are obtained by applying the Eq. (12) and they are depicted in Fig. 5. The dashed line (Hylleraas [13]) slightly overestimates the full line (Silverman *et al.* [12]) in the range 500 to 3000 keV. The relative difference between these curves does not exceed 16.4%, for all the considered energy. It can be seen from Fig. 5 that agreement between the present CB1-4B cross sections (full and dashed curves) and a number of measurements is excellent above 400 keV.

In Fig. 6, we make a comparison of measurements and the theoretical total cross sections for electron capture from $\text{He}(1s^2)$ by Li^{3+} obtained by using Eq. (12) in energy range from 50 to 5000 keV/amu. The present cross sections, the full line (Silverman *et al.* [12]) and the dashed line (Hylleraas [13]), are in excellent agreement with the measurements [16], [31]-[33]. These curves are also very close to each other and the relative difference is up to 16.3%.

The results ($Q_{\text{tot}}^- \simeq Q^-(\Sigma_5) = Q_1^- + Q_2^- + Q_3^- + Q_4^- + 3.049Q_5^-$) for charge exchange in $\text{Be}^{4+} + \text{He}(1s^2)$ collisions at energies from 100 to 3000 keV/amu are depicted in Fig. 7, by the full (Silverman *et al.* [12]) and dashed curves (Hylleraas [13]). The dashed line in this case also

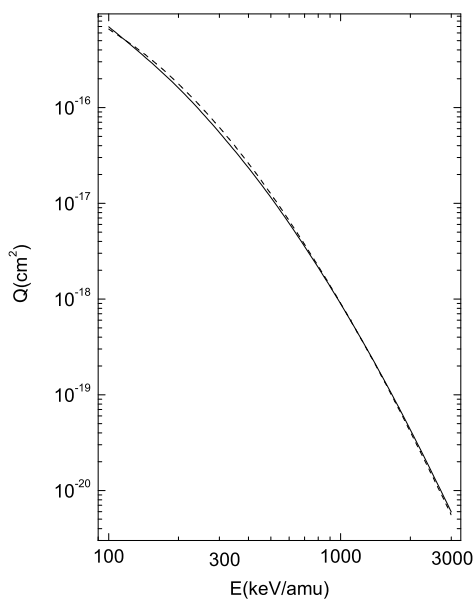


Figure 7. TCS $Q^-(\Sigma_5)$ (in cm^2) as a function of the laboratory incident energy for reaction $\text{Be}^{4+} + \text{He}(1s^2) \rightarrow \text{Be}^{3+}(\Sigma) + \text{He}^+(1s)$. The full and the dashed curves are the present TCS obtained by using the helium ground state wave functions of Silverman *et al.* [12] and Hylleraas [13], respectively.

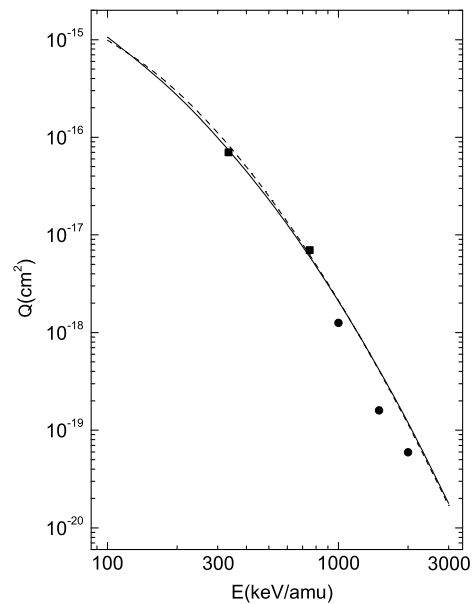


Figure 8. TCS $Q^-(\Sigma_6)$ (in cm^2) as a function of the lab. incident energy for reaction $\text{B}^{5+} + \text{He}(1s^2) \rightarrow \text{B}^{4+}(\Sigma) + \text{He}^+(1s)$. The full and the dashed curves are the present TCS obtained by using the wave functions of Silverman *et al.* [12] and Hylleraas [13], respectively. Exp. data: ■ Dmitriev *et al.* [33]; ● Hippler *et al.* [34].

slightly overestimates full line at energies from 120 to 850 keV/amu, where the relative difference between them does not exceed 13.1%. Unfortunately, no experimental data are available for comparison. The qualitative behaviours of the total cross sections are very similar to those

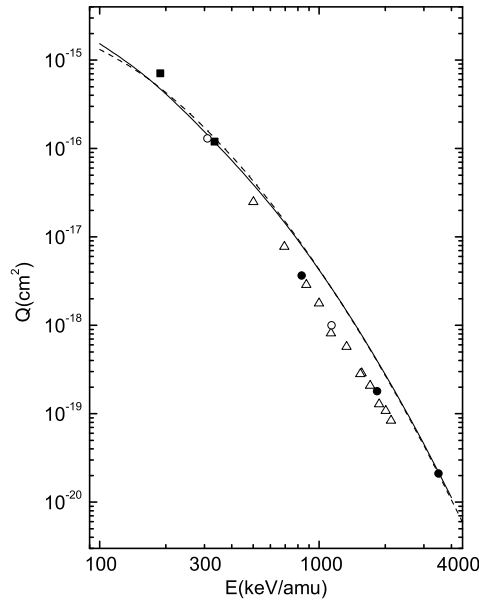


Figure 9. TCS $Q^-(\Sigma_7)$ (in cm^2) as a function of the laboratory incident energy for reaction $\text{C}^{6+} + \text{He}(1s^2) \rightarrow \text{C}^{5+}(\Sigma) + \text{He}^+(1s)$. The full and the dashed curves are the present TCS obtained by using the helium ground state wave functions of Silverman *et al.* [12] and Hylleraas [13], respectively. Experimental data: ■ Dmitriev *et al.* [33]; ● Anholt *et al.* [35]; ○ Graham *et al.* [36]; △ Dillingham *et al.* [37].

corresponding to those for the other considered ions.

Total cross sections for single electron capture in the $\text{B}^{5+} + \text{He}(1s^2) \rightarrow \text{B}^{4+}(nlm) + \text{He}^+(1s)$ process obtained by using $Q_{\text{tot}}^- \simeq Q^-(\Sigma_6) = Q_1^- + Q_2^- + Q_3^- + Q_4^- + Q_5^- + 3.541Q_6^-$ are presented by the full (Silverman *et al.* [12]) and dashed curves (Hylleraas [13]) in Fig. 8. At all the considered energies from 100 to 3000 keV/amu their relative difference is below 13%. The present CB1-4B theory in the prior form describes the experimental data of Dmitriev *et al.* [33] quite successfully, whereas it slightly overestimates the measurements of Hippler *et al.* [34].

A similar trend in behaviour is noticed in the $\text{C}^{6+} + \text{He}(1s^2) \rightarrow \text{C}^{5+}(nlm) + \text{He}^+(1s)$ collisions, where the total cross sections obtained by applying $Q_{\text{tot}}^- \simeq Q^-(\Sigma_7) = Q_1^- + Q_2^- + Q_3^- + Q_4^- + Q_5^- + Q_6^- + 4.035Q_7^-$ at energies from 100 to 4000 keV/amu. These results are shown in Fig. 9 by full (Silverman *et al.* [12]) and dashed (Hylleraas [13]) curves. Now the relative difference is smaller than 11% at energy above 150 keV/amu. It follows from Fig 9. that CB1-4B approximation is in satisfactory agreement with available experimental data [33], [35]-[37]. At higher energies the results from CB1-4B method overestimate experimental data, except those at the largest energy 3500 keV/amu. The discrepancy between the present calculations and the experimental total cross sections for the last two processes at higher energies is not unexpected. Namely, the present CB1-4B method does not include the intermediate ionization channels (electronic continuum intermediate states), which dominate over charge exchange at high energies.

4. Conclusions

We have studied the single charge exchange in collisions between bare nuclei (p, He²⁺, Li³⁺, Be⁴⁺, B⁵⁺ and C⁶⁺) and He targets at intermediate and high impact energies, within the framework of CB1-4B approximation. The results for the prior and post cross sections (both differential and total) for p+He collisions are nearly identical, provided that the repulsive electron-electron interaction $1/r_{12}$ is taken into account in V_f . Moreover, we proved that the contribution from ΔV_{12} increases with augmenting impact energy and decreasing scattering angles. The prior form of the total cross sections has been also calculated by using Silverman *et al.* [12] and Hylleraas [13] wave functions for ground state of helium atom. The relative difference between these results is small, and decreases with increasing the charge of the projectile. On the other side discrepancy between DCS obtained with Silverman *et al.* [12] and Hylleraas [13] wave functions increases with augmenting scattering angle. The contribution from the excited states is more significant at higher than at lower scattering angles. The CB1-4B method is found to be systematically in very good agreement with the available experimental data for p, He²⁺, Li³⁺ projectiles, but for multiply-charged projectiles B⁵⁺ and C⁶⁺ the CB1-4B approximation slightly overestimates measurements at higher impact energy. This behaviour is mainly attributed to the neglect of the intermediate ionization channels which are important in this region.

Acknowledgments

The author thanks the Ministry of Education, Science and Technological Development of the Republic of Serbia for support through Project No. 171020. Thanks are due to Professor Dževad Belkić for helpful discussions and a critical review of the manuscript.

References

- [1] Belkić Dž, Gayet R and Salin A 1979 *Phys. Rep.* **56** 279
- [2] Mančev I and Milojević N 2010 *Phys. Rev. A* **81** 022710
- [3] Mančev I, Milojević N and Belkić Dž 2012 *Phys. Rev. A* **86** 022704
- [4] Mančev I, Milojević N and Belkić Dž 2013 *Phys. Rev. A* **88** 052706
- [5] Dollard D 1964 *J. Math. Phys.* **5** 729
- [6] Cheshire I M 1964 *Proc. Phys. Soc. London* **84** 89
- [7] Belkić Dž 2004 *Principles of Quantum Scattering Theory* (Bristol, Institute of Physics)
- [8] Belkić Dž, Mančev I and Hanssen J 2008 *Rev. Mod. Phys.* **80** 249
- [9] Belkić Dž 2009 *Quantum Theory of High-Energy Ion-Atom Collisions* (London, Taylor & Francis)
- [10] Oppenheimer J R 1928 *Phys. Rev.* **31** 349
- [11] Brinkman H C and Kramers H A 1930 *Proc. K. Ned. Akad. Wet.* **33** 973
- [12] Silverman J N, Platas O, Matsen F A 1960 *J. Chem. Phys.* **32** 1402; Eckart C 1930 *Phys. Rev.* **36** 878
- [13] Hylleraas E 1929 *Z. Phys.* **54** 347
- [14] Shah M B, McCallion P and Gilbody H B 1989 *J. Phys. B* **22** 3037
- [15] Schryber U 1967 *Helv. Phys. Acta* **40** 1023
- [16] Shah M B and Gilbody H B 1985 *J. Phys. B* **18** 899
- [17] Horsdal-Pedersen E, Cocke C and Stockli M 1983 *Phys. Rev. Lett.* **50** 1910
- [18] Berkner K H, Kaplan S N, Paulikas G A and Pyle R V 1965 *Phys. Rev.* **140** A729
- [19] Williams J F 1967 *Phys. Rev.* **157** 97
- [20] Martin P J, Arnett K, Blankenship D M, Kvale T J, Peacher J L, Redd E, Sutcliffe V C, Park J T, Lin C D and McGuire J 1981 *Phys. Rev. A* **23** 2858
- [21] Welsh L M, Berkner K H, Kaplan S N and Pyle R V 1967 *Phys. Rev.* **158** 85
- [22] Löwdin P 1953 *Phys. Rev.* **90** 120
- [23] Mergel V, Dörner R, Jagutzki O, Leneinas S, Nüttgens S, Spielberger L, Unverzagt M, Cocke C L, Olson R E, Schultz M, Buck U, Zanger E, Theisinger W, Isser M, Geiss S and Schmidt-Böcking H 1995 *Phys. Rev. Lett.* **74** 2200
- [24] Hvelplund P, Heinemei J, Horsdal-Pedersen E and Simpson F R 1976 *J. Phys. B* **9** 491
- [25] DuBois R D 1987 *Phys. Rev. A* **36** 2585
- [26] de Castro Faria N V, Freire Jr F L and de Pinho A G 1988 *Phys. Rev. A* **37** 280
- [27] Pivovarov L I, Tabuev V M and Novikov M T 1962 *Sov. Phys. JETP* **14** 20

- [28] Pivovarov L I, Tabuev V M and Novikov M T 1961 *Zh. Eksp. Teor. Fiz.* **41** 26
- [29] Rudd M E, Goffe T V and Itoh A 1985 *Phys. Rev. A* **32** 2128
- [30] Alessi M, Otronto S and Focke P 2011 *Phys. Rev. A* **83** 014701
- [31] Woitke O, Závodszky P A, Ferguson S M, Houck J H and Tanis J A 1998 *Phys. Rev. A* **57** 2692
- [32] Sant'Anna M M, Santos A C, Coelho L F, Jalbert G, de Castro Faria N V, Zappa F, Focke P and Belkić Dž 2009 *Phys. Rev. A* **80** 042707
- [33] Dmitriev I S, Teplova Ya A, Belkova Ya A, Novikov N V and Fainberg Yu A 2010 *Atomic Data and Nuclear Data Tables* **96** 85
- [34] Hippler R, Datz S, Miller P D, Pepmiller P L and Dittner P F 1987 *Phys. Rev. A* **35** 585
- [35] Anholt R, Xu X-Y, Stoller Ch, Molitoris J D and Meyerhof W E 1988 *Phys. Rev. A* **37** 1105
- [36] Graham W G, Berkner K H, Pyle R V, Schlachter A S, Stearns J W and Tanis J A 1984 *Phys. Rev. A* **30** 722
- [37] Dillingham T R, Macdonald J R and Richard P 1981 *Phys. Rev. A* **24** 1237